Available online at http://www.mecs-press.net/ijwmt

Characterization of WLAN System for 60 GHz Residential Indoor Environment Based on Statistical Channel Modeling

Shaela Sharmin[a], Shakil Mahmud Boby[b*]

[a]Department of EEE, Ahsanullah University of Science and Technology, Dhaka-1208, Bangladesh
[b]Department of EEE, Noakhali Science and Technology University, Noakhali-3814, Bangladesh

Abstract

This article investigates on developing a methodology for statistical channel modeling for 60 GHz Wireless Local Area Network (WLAN) system. The most significant characteristics of indoor 60 GHz propagation channels such as large scale propagation path loss, quasi-optical propagation nature, reflection, diffraction, shadowing effect, clustering nature of the channel, effective impact of polarization and necessity of steerable directional antennas are taken into account. This research work has focused on modeling of the 60 GHz WLAN system to estimate the RMS delay spread (RDS) considering both directional and non-directional antennas for residential indoor environment. RDS is a measure of communication channel delay and estimates fading characteristics. Multipath effects and channel deep-fade can be alleviated by minimizing the channel RDS. This research work analyses the RDS characteristics of a living room environment considering two different indoor channel model approaches. Here, the IEEE 802.11ad living room channel model and the Saleh-Valenzuela (S-V) model are considered while developing channel impulse response as well as RDS. The investigations show that highly directional steerable antennas can effectively reduce the channel delay spread. A comparative study between the IEEE 802.11ad and the S-V models has also been performed in the later section.

Index Terms: 60 GHz, mm-wave, channel impulse response, RMS delay spread, IEEE 802.11ad, Saleh-Valenzuela, beamforming, polarization.

1. Introduction

For very high bandwidth wireless communication systems the 60 GHz millimeter (mm)-wave radio

* Corresponding author
E-mail address: shakilmahmud.eee97@gmail.com

technology can be a promising aspirant for future needs. The mm-wave frequency band refers to the frequency band of 30-300 GHz, which in return results in a wavelength of 1-10 mm range; hence it is named mm-wave. The globally available 60 GHz unlicensed band can be a significant solution to meet the uprising demand for short-range multi-gigabit data rate links [1, 2]. The main advantages of 60 GHz frequency spectrum are, it has large bandwidth which permits high data rate and has a short wavelength that leads to small antenna dimensions. Furthermore, this frequency spectrum has been allocated for unlicensed wireless systems by the Federal Communications Commission (FCC), which can be a reasonable solution for short-range and high data rate indoor wireless communications. In comparison with 2.4 GHz and 5 GHz legacy Wireless Local Area Network (WLAN) systems, the carrier frequency for 60 GHz WLAN system has increased more than 10 times which leads to qualitative changes in signal propagation properties. The small wavelength of 60 GHz band results in significantly larger free space path loss assuming constant gain antennas, a higher penetration loss, greater attenuation and significant shadowing effect due to obstructing objects in the propagation path [3]. The smaller wavelength at higher frequencies limits the propagation distance. However, this can be proved advantageous as the system will experience less interference from other nearby users operating at the same frequency which in turn will allow for a larger potential of frequency reuse.

The propagation characteristics of the 60 GHz band are quite different from conventional 2.4 GHz and 5 GHz frequency bands [3]. Larger obstacles in the propagation path help to form a sharp shadow zone. This will cause diffraction and an insignificant propagation mechanism [4]. As most of the materials undergo high penetration loss at 60 GHz, multipath components propagating through wall and other objects will experience lower power. In order to overcome this degradation of power, highly steerable directional antennas with adaptive beamforming algorithm techniques are required to establish a communication link between transmitter (Tx) and receiver (Rx) [5]. 60 GHz propagation channel employs quasi-optical nature [3] as it tends to behave like a light wave with higher frequencies. Due to this nature, waves tend to propagate in a straight line. As angle of diffraction and size of wavelength possess directly proportional relationship, propagation due to diffraction is insignificant and not viable at 60 GHz frequency range [7, 18]. Most of the transmitted power is propagated through Line-of-Sight (LOS) or lower order reflection paths [3, 6]. This phenomenon gives a hint that higher-order reflections can be neglected. Polarization is another significant characteristic that must be taken into consideration during channel modeling [6]. With the attribution of highly directional steerable antennas, only a single LOS or Non-Line-of-Sight (NLOS) path is essentially used to transmit signal and at the receiver end, even NLOS signals remain strongly polarized.

The utmost objective of this paper is to develop a methodology for the development of 60 GHz WLAN system, which has taken into account all the characteristics discussed above. When detailed knowledge of the propagation channel is not available, the statistical channel model should be used [3]. For channel modeling at 60 GHz, the clustering approach is followed. RMS delay spread (RDS) is determined considering both LOS and NLOS situations along with different beamwidths at transmitter and receiver sides for residential indoor environment. As the IEEE 802.11ad model is based on a mixture of ray tracing and measurement-based statistical modeling techniques, measurements are taken with considering this multiple-input multiple-output (MIMO) model [7]. This research work is organized in the following ways. Section 2 describes the necessity, merits and demerits of 60 GHz system. Section 3 describes the properties of indoor channel modeling at the 60 GHz frequency spectrum. Section 4 narrates the mathematical structure of the IEEE 802.11ad model. Section 5 considers a living room scenario and determines intra-cluster RMS delay spread considering both polarization and without polarization scenarios. Section 6 describes the Saleh-Valenzuela (S-V) model. Basic differences between the IEEE 802.11ad model and the Saleh-Valenzuela model are also discussed in section 7. Finally, section 8 concludes the research work.

2. Necessity, Merits and Demerits of 60 GHz System

60 GHz band is the utmost solution to spectrum shortage. It is basically the backward-compatible extension

of the IEEE 802.11-2012 standard. This extension adds a new MAC/PHY to provide short-range, high capacity links in 60 GHz unlicensed band. As antenna size is directly related to the wavelength, multiple antenna elements can be integrated onto a small area. Because of high data rate of 6.75 Gbps speed, device-to-device, in-flight [8] and in-car [9] communications are possible. For wireless short-range, high-precision localization systems, fifth-generation (5G) broadband cellular communication, wireless backhaul connections and high data rate inter-chip communication [10], this 60 GHz mm-wave system can be of great use. License-free 60 GHz radio wave has unique characteristics in comparison with traditional 2.4 GHz or 5 GHz license-free radio wave which give operational advantages of 60 GHz radio waves which are not found in other wireless systems [27, 28]. Shannon's law states that with the increase of channel bandwidth, maximum possible data rate also increases.

$$\text{Shannon Capacity} = \text{Channel BW} \times \log(\frac{\text{Power}}{\text{Noise}}) \tag{1}$$

It is seen from (1) that a much higher data rate can be achieved by 60 GHz band. Besides, by using highly directional antennas maximum power can be transferred. The very narrow beam associated with 60 GHz allows multiple 60 GHz radios to be installed on the same location. In addition to high data rate, energy propagation at 60 GHz exhibits many other benefits such as highly secure operation, virtually interference-free functions and ability to the high level of frequency reuse [28].

60 GHz frequency band is prone to higher path loss. A convenient way to express free space path loss equation is

$$\text{FSPL(dB)} = 20\log_{10}\left(\frac{4\pi df}{c}\right) \tag{2}$$

Where, c denotes the speed of light and d represents distance between the antennas. It is seen from (2) that free space path loss highly depends on carrier frequency (f). Fig. 1 depicts that for 60 GHz band path loss increases drastically. This feature limits the distance that can be covered by this spectrum. It mainly affects low power transmission.
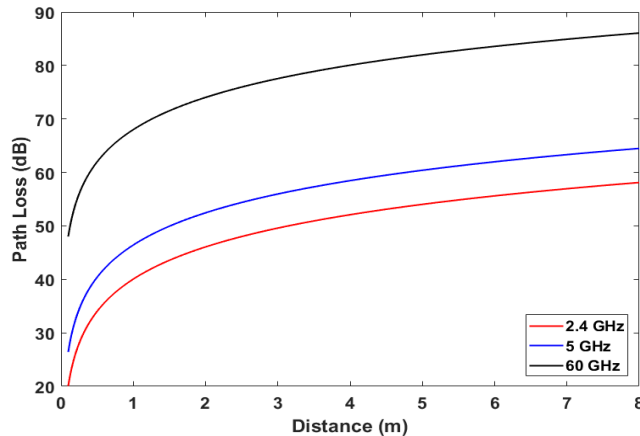

Fig. 1. Free space path loss model for 2.4 GHz, 5 GHz and 60 GHz band.

In practical cases, the path loss is not constant for a given Tx-Rx distance as propagation paths will be different each time for a given distance. Some will face increased loss and some will face fewer obstructions which will be resulting in received power mismatch. This phenomenon is called slow fading. Even after path loss and slow fading have been predicted for particular locations, there still remains significant variations in the received signal when an antenna is moved over relatively small distances. It is due to the fact that the received signal is the summation of different rays coming from different directions. Since different rays may have different phases, the amplitude may vary in a wide range of around 30-40 dB. This is called fast fading [29] and this phenomenon can only be usefully predicted by statistical means.

3. Indoor Channel Model Properties at 60 GHz

Indoor channel modeling exhibits several unique characteristics for 60 GHz frequency band, e.g. reflection properties from the different surface, diffraction, shadowing property, polarization characteristics etc. Some of these properties will be discussed in this section. Power delay profile (PDP), RMS delay spread, and Rician-K factor are some parameters of statistical channel modeling. The communication path will be faster if RDS is reduced. RDS highly depends on the side lobe level (SLL) and beamwidth of antenna radiation pattern [15]. Some of the factors that affect the RDS of an indoor wireless propagation channel are shown in Fig. 2. Reference [19] describes the effect of SLL on RDS for the IEEE 802.11ad living room channel model. It is found that, reduced SLL of radiation pattern can effectively reduce the RDS [19]. Hence, the effect of SSL is skipped here.
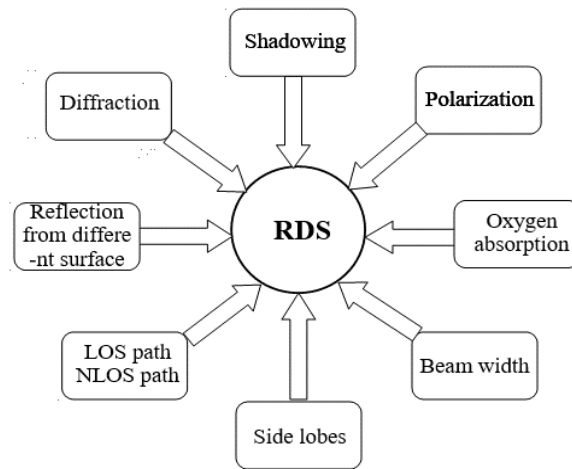

Fig. 2. Some of the factors that affect RMS delay spread (RDS) at indoor wireless propagation channel.

3.1. Analysis of reflection properties from different surfaces

For ideal reflections, each propagation path would include only a single ray. But according to experimental investigations explained in [6], each reflected path actually consists of a number of rays. Because of the fine structures of the reflected surfaces, these rays are closely spaced to each other in time and angular displacements. Hence, the clustering approach is suitable for channel modeling of 60 GHz wave propagation, where each cluster consists of corresponding LOS or NLOS reflected paths [18]. A cluster comes from various reflected areas, such as walls, furniture and anything else present in the environment of propagation. Hence, the size of clusters depends on the nature and layout of objects that are distributed in the room, which in turn

affects the RDS of an indoor wireless communication channel [13, 18]. Reflectivity of building material is an important factor that influences RDS. In reference [30], it is found that, small room with metal walls exhibits higher RDS than a much larger auditorium room with walls covered by wood and acoustically soft material.

To get the maximum directivity gain the beam of transmitter and receiver has to be pointed to each other. Hence, the transmission path is needed to be LOS for the usage of narrow beam in the 60 GHz link. However, a 60 GHz channel does not only rely on the LOS transmission path but also able to utilize the NLOS transmission path from the reflected signal. The higher-order reflected signals reduce the received signal power. Therefore, the reflected signal, especially the first-order and second-order reflections have the potentiality of becoming an alternative transmission path where the LOS path is unavailable.

3.2. Analysis of diffraction at 60 GHz

Reflected, diffracted and scattered waves from the nearby objects result in multipath fading effect which in turn influence the performance of indoor wireless communication system. Reflection is the dominating factor that affects the channel delay at 60 GHz. Diffraction occurs when the bending of waves takes place in the same medium. As the frequency increases, the significance of diffraction decreases. Because of sharp shadow zone, diffraction at 60 GHz is an insignificant property [4, 7, 18]. If the wavelength is smaller in comparison to the gap size, diffraction will be very little in amount and outgoing waves will spread less. Hence, diffraction at 60 GHz can be ignored.

3.3. Shadowing effect by human body

Because of small wavelength and the usage of narrow beams in 60 GHz communications, data transmission becomes very vulnerable to blockage from obstacles such as humans. Path loss can be increased by the presence of body shadowing which can exceed the fading margin of the link. This phenomenon will affect RDS of indoor wireless communication. A transient blockage resulting from a human walking across the link causes a temporary link disruption. On the other hand, a person standing in between the link for a long duration might cause a permanent blockage resulting in long-term link disruption. Hence, it is necessary to characterize and categorize the human blockage in 60 GHz links based on human activity and explore its effect on the link quality performance so that by analyzing the characteristic of blockage, a 60 GHz device can identify the blockage type and can determine an action that has to be taken to circumvent the blockage. Relay and fast session transfer (FST) are some of the mechanisms for addressing the long term blockage issue. The IEEE 802.11ad model has the above-mentioned mechanisms in addressing human blockage [11].

3.4. Polarization effect for NLOS ray

Reflection and scattering interactions with the environment and multi-path propagation are the main causes of the cross-polarized signal. Unlike legacy 2.4 GHz and 5 GHz WLAN systems, 60 GHz channel modeling requires detailed support of polarization characteristics of the antenna and channel.

The degradation due to polarization for first and second-order reflections for office environments can be as much as 10-20 dB at 60 GHz [6]. Cross polarization values for office and conference room scenario have been found to be 6.6 dB and 6.3 dB respectively at 5.2 GHz WLAN system [16]. By comparing the mentioned values it can be said that cross-polarization values are more significant at higher frequencies than lower frequencies. At 60 GHz, reflection characteristics of the wave largely depend on the reflecting material and incident wave polarization. In order to change the reflection characteristic of a wave, the polarization of that particular wave should be changed. Appropriately used polarization can cause a reduction of channel RMS delay spread which in turn resulting in high data rate communication. Different polarization techniques can be used in mm-wave frequency antennas such as a dual-polarized antenna or circularly polarized antenna [17].

4. General Mathematical Structure of IEEE 802.11ad Channel Model

The IEEE 802.11ad standard is based on the results of experimental and statistical data at 60 GHz and describes the channel models for WLAN system [6]. This model [6, 7] generates impulse response of the channel which supports both with and without antenna polarization characteristics. Beamforming performance is also considered in the model. The impulse response of the model with polarization characteristics can be expressed as [6, 7]

$$h(t,\varphi_{tx},\theta_{tx},\varphi_{rx},\theta_{rx}) = \sum_i H^{(i)} C^{(i)}(t - T^{(i)}, \varphi_{tx} - \phi_{tx}^{(i)}, \theta_{tx} - \Theta_{tx}^{(i)}, \varphi_{rx} - \phi_{rx}^{(i)}, \theta_{rx} - \Theta_{rx}^{(i)}) \qquad (3)$$

Where,

$h()$ = generated channel impulse response, which is a sum of multiple channel clusters;

$t, \varphi_{tx}, \theta_{tx}, \varphi_{rx}, \theta_{rx}$ = time and azimuth and elevation angles at the transmitter and receiver respectively;

$T^{(i)}, \phi_{tx}^{(i)}, \Theta_{tx}^{(i)}, \phi_{rx}^{(i)}, \Theta_{rx}^{(i)}$ = time-angular coordinates of the i-th cluster;

$H^{(i)}$ = 2 x 2 matrix gain of the i-th cluster describing its polarization characteristics [Gain of the channel impulse response is merged in to $H^{(i)}$];

$C^{(i)}$ = channel impulse response for the i-th cluster which can be expressed as [6, 7]

$$C^{(i)}(t,\varphi_{tx},\theta_{tx},\varphi_{rx},\theta_{rx}) = \sum_k \alpha^{(i,k)} \delta(t - \tau^{(i,k)}) \delta(\varphi_{tx} - \varphi_{tx}^{(i,k)}) \delta(\theta_{tx} - \theta_{tx}^{(i,k)}) \delta(\varphi_{rx} - \varphi_{rx}^{(i,k)}) \delta(\theta_{rx} - \theta_{rx}^{i,k}) \qquad (4)$$

Here,

$\delta()$ = Dirac delta function;

$\alpha^{(i,k)}$ = amplitude of the k-th ray of the i-th cluster;

$\tau^{(i,k)}, \varphi_{tx}^{(i,k)}, \theta_{tx}^{(i,k)}, \varphi_{rx}^{(i,k)}, \theta_{rx}^{i,k}$ = relative time-angular coordinates of the k-th ray of the i-th cluster;

It is found that, this model generates a channel realization considering space, time, amplitude, phase, and polarization characteristics of all rays [6]. Azimuth and elevation angles for both Tx-Rx sides are considered for spatial characterization of the rays. Three basic propagation model scenarios, i.e. conference room, cubical and living room environment can be evaluated using the IEEE 802.11ad model [6].

5. Residential Indoor Living Room Scenario

This section describes channel realization characteristics of a living room scenario using the IEEE 802.11ad standard. The IEEE 802.11ad living room model considers the floor plan [20] scenario according to [21]. Fig. 3 depicts simplified model of living room used in realizing the channel model [6, 21].
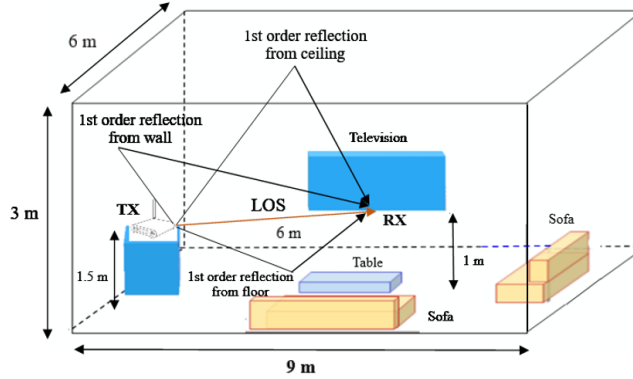
Fig. 3. 3D simplified model of the living room for the IEEE 802.11ad channel model (adopted from ref. [3]).

Simulation results have been performed considering living room dimensions of 9m x 6m x 3m (L x W x H). In the simulation scenario, communication can be established between a router and a smart television (TV). Transmitted data will be received by the TV while necessary. The TV is placed in the middle of one of the walls. Distance between transmitter and receiver has considered to be 6 m for simulation purposes.

Table 1. Intercluster structure

Types of clusters	Number of clusters
LOS path	1
First-order reflections from the wall	3
First-order reflections from the ceiling	1
First-order reflections from floor	2

A ray-tracing model for the living room has been used to generate multiple realizations of the LOS and first-order reflected clusters to investigate the intracluster structure for the considered environment.

The polarization characteristics of the model are proposed at the cluster level. Because of the quasi-optical nature, the incidence of different reflected waves occur almost in the same region. Hence, it seems that this group of reflected waves is acting like a single wave. For this, it has been assumed that all rays consisting of one cluster have approximately the same polarization properties.

From Table 1, it can be seen that all the clusters are divided into four groups, where clusters in the same group have similar properties. Average RDS for this specific living room scenario has been determined considering different beamforming angles for both transmitter and receiver antennas using the IEEE 802.11ad model which constitutes a mix of measurement based stochastic parameters, ray tracing, empirical distributions and theoretical models [12]. Both LOS and NLOS sub-scenarios are supported by this channel model.

RDS is a measure of how the multipath power in the channel is spread over the delay. It depends on several factors, e.g. propagation channel, shadowing, type of antennas, polarization for the antennas and signal processing techniques that are applied to the transmitted signal.

Mean excess delay,

$$\bar{\tau} = \frac{\sum_k a_k^2 \tau_k}{a_k^2} = \frac{\sum_k P(\tau_k)\tau_k}{\sum_k P(\tau_k)} \tag{5}$$

RMS delay spread,

$$\tau = \sqrt{\overline{\tau^2} - \bar{\tau}^2} \tag{6}$$

Where,

$$\overline{\tau^2} = \frac{\sum_k a_k^2 \tau_k^2}{\sum_k a_k^2} = \frac{\sum_k P(\tau_k)\tau_k^2}{\sum_k P(\tau_k)} \tag{7}$$

Here, τ_k denotes channel delay of the k-th path while $P(\tau_k)$ and a_k denote the power and amplitude respectively. Above equations (5) to (7) do not rely on the absolute power level of $P(\tau)$, but on the relative amplitudes of the multipath components in $P(\tau)$.

The probability of arrival of different rays at the receiving end for simulation purposes are enlisted in Table 2. Only first-order reflections from different surfaces are considered here and the shadowing effect is neglected.

Table 2. Spread probability of arrival of different types of ray for the Living Room Simulation Model

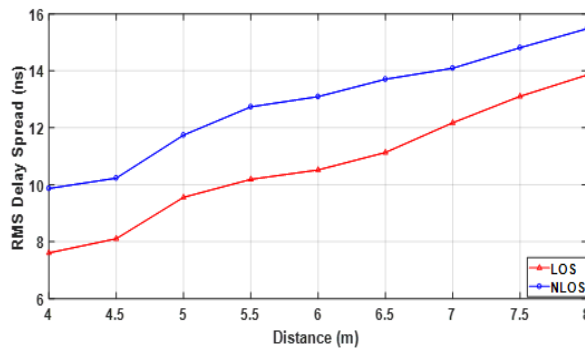| Types of rays	Probability of arrival at the receiver
1st order reflections from the ceiling	1
1st order reflections from floor	0.5
1st order reflections from walls	0.66

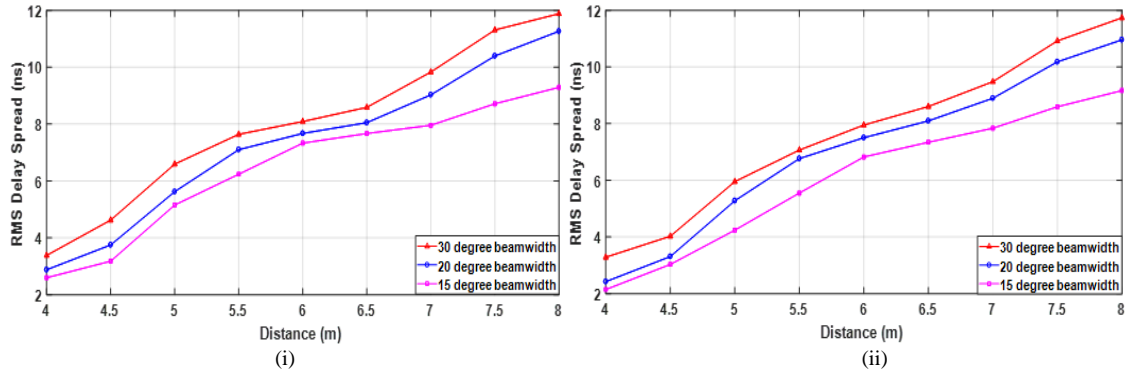Fig. 4. RDS for Omni-directional antennas for LOS and NLOS signals

Fig. 5. RDS for LOS signal considering directional steerable antennas (i) without applying the Tx-Rx polarization vector and (ii) with applying antenna polarization.

When the LOS path is present, the antennas should be steered along the LOS path in order to get the maximum received signal power. For the NLOS environment, transmitter and receiver antennas apply beamforming algorithms and steer their beam toward the best-reflected path (cluster) to establish a higher data transmission communication link. In such an approach, the transmitter and receiver antennas filter out only one spatial cluster that's why the characteristics of the beamformed channel directly depend on the intracluster parameters [7].

Fig. 4 depicts average RDS for LOS and NLOS signal while Omni-directional antennas are used in both transmitting and receiving stations. Simulations have been performed considering a variable transmitter and receiver distance of 4-8 m as their positions can be varied. Due to the presence of multipath, indoor path loss can change dramatically with the variation of either time or position within a certain range. If the distance between transmitter and receiver is considered to be 6 m (earlier declared in the living room model), average RDS for this distance can be determined from (6). For NLOS and LOS signals, average RDS becomes 12.7332 ns and 10.1878 ns respectively for 6 m Tx-Rx distance.

With the application of highly directional steerable antennas at both ends, RDS for this case scenario can be minimized. In later section several simulations have been performed considering directional antennas at both ends of the communication channel and the significance of polarization at 60 GHz has also been monitored.

Fig. 5 shows that the average RMS delay spread reduces with narrower beamwidth. Simulation has been performed for three different antenna beamwidths, e.g. 30 degree, 20 degree and 15 degree considering both without the Tx-Rx polarization vector (Fig. 5(i)) and with specific antenna polarization (Fig. 5(ii)). Horizontal linear polarization (HLP) has been applied at both transmitter and receiver ends. By comparing Fig. 5(i) and Fig. 5(ii) it can be concluded that, if polarization is applied appropriately, channel delay spread can be minimized up to a certain level; hence faster communication will be possible.
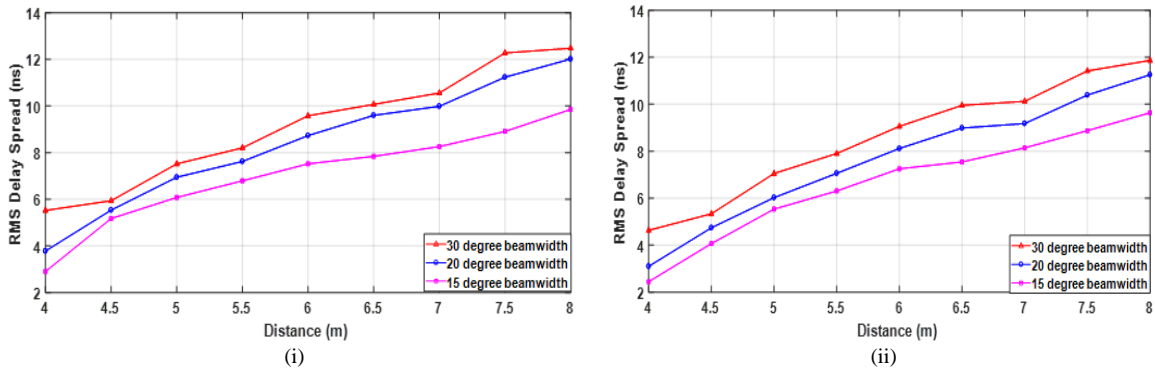
Fig. 6. RDS for NLOS signal considering directional steerable antennas (i) without applying the Tx-Rx polarization vector and (ii) with applying antenna polarization.

It is obvious that NLOS signals will possess more time of arrival rate than LOS signals. Simulations for NLOS rays have also been performed in this section. Both polarization and without polarization conditions were taken into account. Fig. 6(i) shows graphs of average RDS for different antenna beamwidth angles without applying any specific antenna polarization for the NLOS signals, whereas Fig. 6(ii) exhibits average RDS graphs for the same scenario along with appropriately applied HLP at both Tx-Rx ends.

Table 3 summarizes all the findings of simulation works. As 6 m distance has been considered between transmitter and receiver, average RDS for this particular distance has been mentioned only. Literature reveals that RDS values at 60 GHz had remained within the range of 15 ns ~ 45 ns for small rooms and within the range of 30 ns ~70 ns for the large indoor environment [27].

Simulation results show that narrower beamwidth along with appropriately applied antenna polarization reduces RDS. Narrower beam means more focused propagation wave which in turn will reduce transmission path loss. This results in higher received power and reduced time delay. Hence the necessity of narrower beamwidth along with apposite antenna polarization is very essential in order to make communication possible at 60 GHz frequency range.

Table 3. Various intracluster average RMS delay spread for 6 m Tx-Rx distance.

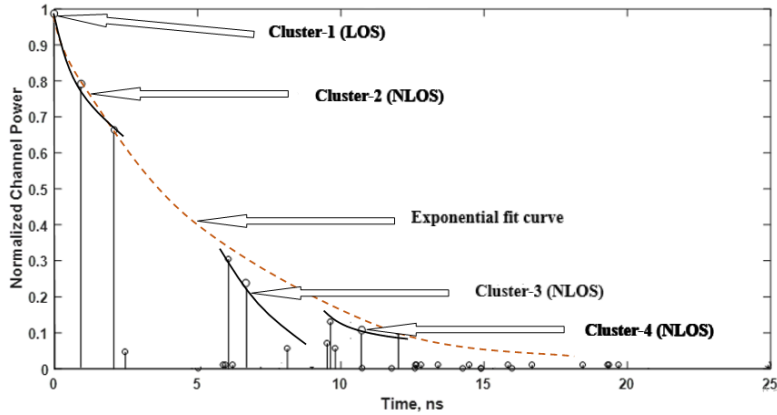| Types of Communication	Polarization (both on Tx-Rx ends)	Tx Beam angle (degree)	Rx Beam angle (degree)	RMS delay spread (ns)
LOS	Not applied	30^0	30^0	8.0890
		20^0	20^0	7.6706
		15^0	15^0	7.2501
	Applied	30^0	30^0	7.9477
		20^0	20^0	7.5014
		15^0	15^0	6.8206
NLOS	Not applied	30^0	30^0	9.5777
		20^0	20^0	8.7287
		15^0	15^0	7.5192
	Applied	30^0	30^0	9.0568
		20^0	20^0	8.1117
		15^0	15^0	7.3286

Fig. 7. Power Delay Profile (PDP) of a receiver in the living room of Fig. 3.

The power delay profile (PDP) for this living room case environment is also simulated. PDP specifies the energy density of a signal received at the receiving end through multipath channel as a function of time delay. Fig. 7 shows the excess delay at the receiving station in the living room. Tx-Rx distance was considered 8 m in this case. From Fig. 7 it is clear that the excess delay follows the exponential decay curve. PDP in the living room consists of several narrow peaks and an exponentially decaying power distribution. Arrival times of some clusters (LOS and NLOS) are also shown in the Fig. 7. Here the LOS ray is considered as Cluster-1.

6. Saleh-Valenzuela (S-V) Model

Saleh-Valenzuela (S-V) model is another popular and widely accepted model [13] based on indoor multipath propagation measurements. This model describes the stochastic properties of the arrival delays and amplitudes of resolvable multipath components (MPCs) in indoor wireless transmission systems. Just like IEEE 802.11ad model, S-V model is one of the statistical channel models suitable for frequency band of 57-66 GHz. Both the S-V model and the IEEE 802.11ad standards define MAC and PHY layers for operating in 60 GHz band capable of multi-Gbps throughput. Both the standards are designed for short range communication and support both LOS and NLOS. If quantitative and qualitative analysis are considered i.e. network architecture, MAC/PHY mechanism, beamforming procedures etc. both of the models exhibit almost similar performance [31]. Hence, S-V model is considered to be compared with the IEEE 802.11ad standard in terms of RDS.

The S-V model shows that, rays are likely to arrive in closely spaced groups, or in clusters. It means that, there are multiple clusters, each with multiple rays in the delay profile. From PDP it is found that, the second clusters are attenuated in amplitude and the rays within each cluster decay with time as well. In this way, a channel comprises a random spatial distribution of ray clusters. S-V model was used as the basis for the IEEE 802.15.3a model [24, 25]. This standard was developed to compare standardization proposals for high data rate wireless personal area networks (WPANs). S-V model was mainly inspired by the pioneering work of Turin, who postulated that received signal of the wideband wireless communication system can be written as a sum of several undistorted multipath components of the transmitted signal [22, 23]. Poisson distribution is used to describe the arrival times of rays and clusters [14, 22, 23]. The delay of each path is spaced in an arbitrary manner. A distribution of intercluster arrival times and a distribution of inter-ray arrival times can be expressed by the following two exponential distribution equations respectively [14, 22, 23]

$$f_{T_i}(T_i \mid T_{i-1}) = \Lambda \exp[-\Lambda(T_i - T_{i-1})] \quad ; i = 1, 2, \ldots \ldots \tag{8}$$

And,

$$f_{\tau_{k,i}}(\tau_{k,i} \mid \tau_{k-1,i}) = \lambda \exp[-\lambda(\tau_{k,i} - \tau_{k-1,i})] \qquad ; k = 1, 2, \ldots \ldots \tag{9}$$

Where,

$\tau_{k,i}$ = arrival time of the k-th ray in the i-th cluster;

T_i = arrival time of the first ray in the i-th cluster;

Λ = cluster arrival rate;

λ = ray arrival rate at each cluster;

Let $\beta_{k,i}$ and $\theta_{k,i}$ denote amplitude and phase of the k-th ray in the i-th cluster respectively. The channel impulse response can be expressed as

$$h(t) = \sum_{i=0}^{\infty} \sum_{k=0}^{\infty} \beta_{k,i} e^{j\theta_{k,i}} \delta(t - T_i - \tau_{k,i}) \tag{10}$$

Where, $\theta_{k,i}$ is a random variable that is uniformly distributed over $(0, 2\pi)$ and $\beta_{k,i}$ is an independent random variable with the following Rayleigh distribution

$$f_{\beta_{k,i}}(\beta_{k,i}) = \left(\frac{2\beta_{k,i}}{\overline{\beta_{k,1}^2}}\right) e^{-\frac{\beta_{k,i}^2}{\overline{\beta_{k,1}^2}}} \tag{11}$$

Here, $\overline{\beta_{k,1}^2}$ is the average power of the k-th ray in the i-th cluster, which is given as

$$\overline{\beta_{k,1}^2} = \overline{\beta_{0,0}^2} e^{-\frac{T_i}{\Gamma}} e^{-\frac{\tau_{k,i}}{\Upsilon}} \tag{12}$$

Where, Γ and Υ denote time constants for exponential power attenuation in the cluster and ray respectively, while $\overline{\beta_{0,0}^2}$ denotes the average power of the first ray in the first cluster.

Though an infinite number of clusters and rays are presented in the channel impulse response of (10), there exists only a finite number of the non-negligible number of clusters and rays in practice. Therefore, the number of clusters and rays is reduced to I and K, respectively. A log-normal random variable X, that is, $20\log_{10}(X) \square N(0, \sigma_x^2)$ can be introduced in impulse equation in order to observe the effect of long-term fading.

$$h(t) = X \sum_{i=0}^{I} \sum_{k=0}^{K} \beta_{k,i} e^{j\theta_{k,i}} \delta(t - T_i - \tau_{k,i}) \tag{13}$$

Simulations have been performed to plot the distributions of cluster arrival times, ray arrival times, the channel impulse response of the S-V channel and channel power distribution respectively. Parameters used in this model are based on LOS and NLOS (4-10 m) channel measurements reported in [24, 25, 26]. Some of the values are modified envisaging the living room scenario proposed in this research work. Considered values of

different parameters are enlisted in Table 4. The range of RDS is also calculated for this model.

Table 4. Parameters used in channel realization

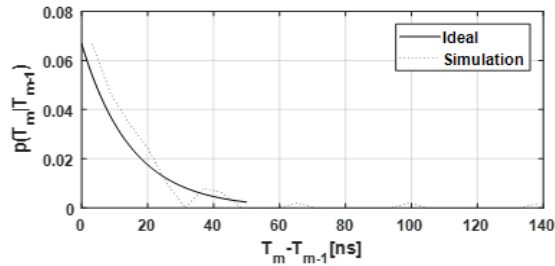| Description	Units	Values
Cluster arrival rate	1/ns	0.0667
Ray arrival rate	1/ns	2.1
Cluster decay factor	ns	14
Ray decay factor	ns	7.9
Log normal shadowing term	dB	3

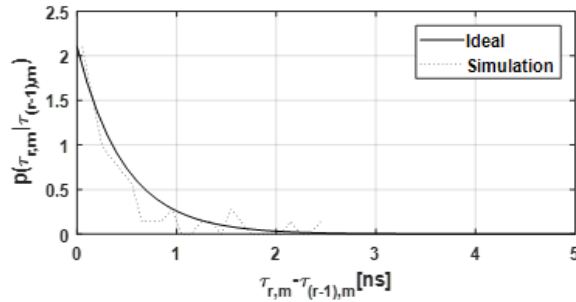Fig. 8. Distribution of cluster arrival time, $\Lambda = 0.0667$ ns^{-1}

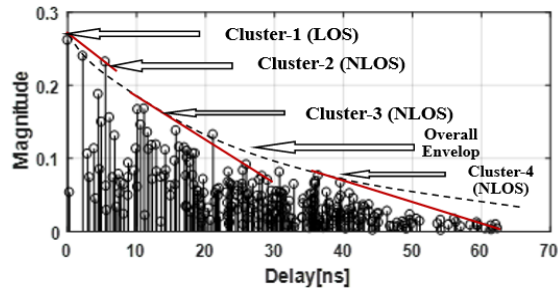Fig. 9. Distribution of ray arrival time, $\lambda = 2.1$ ns^{-1}.
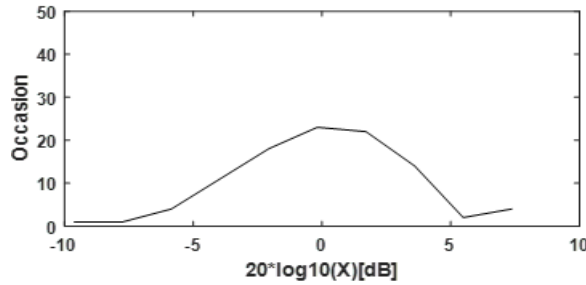

Fig. 10. Generated channel impulse response.

Fig. 11. Log-normal distribution, $\sigma_x = 3$dB.

From the simulation, it has been found that for the same parameter values, the RDS will be smaller in LOS condition than for NLOS condition. Since the NLOS case produces more arriving rays in the receiver than the LOS case, this results in an increase of RDS. It is noteworthy to mention that due to the difference in multipath effects and overall received power, the values of RDS in LOS and NLOS scenarios are not precisely comparable. From different simulation results, it has been found that RDS remains within a range of 8 ns~16 ns considering different parameter values mentioned in Table 4. Fig. 8 and Fig. 9 show the distributions of cluster arrival times and ray arrival times respectively. Each of them possesses exponentially decreasing characteristics with time of arrival (TOA).

Fig. 10 shows the random realization of the channel impulse response of the S-V model considering both LOS and NLOS rays. PDP for small scale channel modeling can be obtained by taking the spatial average of the channel's baseband impulse over a local area. The impulse response of the multipath channel is an exponentially decaying curve just like PDP. Cluster-1 is considered as the LOS ray. Channel power distribution for this scenario is obtained by simulating 100 channels. From Fig. 11 it is clear that the channel power follows a log-normal distribution.

Studies found that for generalized S-V model RMS delay spread will remain within a range between several tens to several hundreds of nanoseconds [15]. In indoor cases, RDS is supposed to be lower than 100 ns. If channel parameters are changed, variation in RDS is observed. However, the results found in this section agree with the literature and channel models in IEEE standards.

7. Comparative Study Between IEEE 802.11ad and S-V Models

Propagation characteristics of the mm-wave band are quite different from frequency bands lower than 6 GHz. Two popular statistical channel models, IEEE 802.11ad and S-V model have been discussed in section 5 and section 6 respectively for 60 GHz indoor wireless communication system. Average RDS for an indoor living room scenario has been determined using both of these models.

The IEEE 802.11ad model is a composition of ray tracing, empirical distribution and theoretical model. Cluster delays as well as angles are determined using ray tracing. Again using empirical distribution, amplitude and intracluster angular distribution of the reflected rays can be determined. Along with these, theoretical models are required to find out polarization properties. In section 5, it has been found that highly steerable narrow beamwidth antenna along with due antenna polarization can reduces average RDS of multipath propagation of 60 GHz WLAN channel which in turn increases bit rate and decreases bit error rate (BER). Though because of multipath propagation RDS may vary within a certain range, it has been evident that rays of LOS path possess lower RDS in comparison with the NLOS path.

The S-V model is a single-input multiple-output (SIMO) model that only models direction of arrival (DOA). In contrast, the IEEE 802.11ad model develops delay, the direction of departure (DOD) and DOA for clusters using empirical distributions of different types of 1st and 2nd order clusters, streaming from different surfaces.

The S-V model relies on the assumption that the delay and angular domains can be modeled independently. For the 60 GHz channel, this assumption might not be valid [18]. Instead, it will be efficient to develop either a joint model considering angular-delay distribution or to use a deterministic approach based on ray tracing which is accomplished in the IEEE 802.11ad model. An extended version of the Triple Saleh-Valenzuela model is IEEE 802.15.3c standard. Though the communication procedures and transmission delay in both standards are very similar, the IEEE 802.11ad has emerged as the choice for multi-Gbps indoor WLAN communication system over the S-V model because of its back compatibility with Wi-Fi and other compositions such as coexistence features, relay support, FTS mechanism etc.

8. Conclusion

This research work represents delay characteristics of a 60 GHz indoor WLAN channel model using both IEEE 802.11ad and S-V models. Simulation results discussed in this article confirmed that practice of steerable directional antennas with narrow beamwidth and appropriate antenna polarization can reduce RDS of 60 GHz wireless indoor fading channel. Hence, by applying the beamforming algorithm both at Tx-Rx ends, 60 GHz short-range indoor communication can be effectively established. Average RDS obtained from the IEEE 802.11ad model and the S-V model exhibits slight differences in magnitude. The differences in RDS of the two sections were mainly due to the difference in room dimensions, Tx-Rx antenna height difference and multipath environments. According to the quantitative performance analysis, both the IEEE 802.11ad and the S-V models have almost the same performance in terms of throughput and delay. However, qualitative comparison shows that IEEE 802.11ad is more robust than the S-V model because IEEE 802.11ad has additional features of coexistence and backward compatibility. Hence, the IEEE 802.11ad standard seems to be more promising network for multi-Gbps WLAN communications in the future. Integration of 60 GHz band to 5G networks can be an auspicious thing, as already existing 60 GHz research and standardizations can help in defining new schemes for 5G networks.

References

[1] M. Nedil, A. M. Habib, A. Djaiz and T. A. Denidni, "Design of new mm-wave antenna fed by CPW inductively coupling for mining communication," in the 2009 IEEE Antennas and Propagation Society International Symposium, pp. 1-4, 1-5 June, 2009 Charleston, SC, USA.

[2] P. F. M. Smulders, "60 GHz radio: prospects and future directions," in proceedings of IEEE Symposium Benelux Chapter on Communications and Vehicular Technology, pp. 1–8, 13 November, 2003 Eindhoven, The Netherlands.

[3] H. Xu, V. Kukshya, and T. S. Rappaport, "Spatial and temporal characteristics of 60-GHz indoor channels', IEEE Journal on Selected Areas in Communications, Vol. 20, No. 3, pp. 620–630, 2002.

[4] C. Gustafson and F. Tufvesson, "Characterization of 60 GHz shadowing by human bodies and simple phantoms", Radioengineering, Vol. 21, No. 4, pp. 979-984, 2012.

[5] X. Zhu, A. Doufexi and T. Kocak, "Beamforming performance analysis for OFDM based IEEE 802.11ad millimeter-wave WPANs", in the 8th International Workshop on Multi-Carrier Systems and Solutions (MC-SS), pp. 1-5, 3-4 May, 2011 Herrsching, Germany.

[6] A. Maltsev, E. Perahia, R. Maslennikov, A. Sevastyanov, A. Lomayev and A. Khoryaev, "Impact of polarization characteristics on 60 GHz indoor radio communication systems", IEEE Antennas and Wireless Propagation Letters, Vol. 9, pp. 413 – 416, 2010.

[7] A. Maltsev, R. Maslennikov, A. Lomayev, A. Sevastyanov and A. Khorayev, "Statistical channel model for 60 GHz WLAN systems in conference room environment", Radioengineering, Vol. 20, No. 2, pp. 409-422, 2011.

[8]   M. Beltran, R. Llorente, R. Sambaraju, and J. Marti, "60 GHz UWB over-fiber system for in-flight communications", i n the 2009 IEEE MTT-S International Microwave Symposium Digest, pp. 5–8, 7-12 June, 2009 Boston, MA, USA.

[9]   M. Peter, R. Felbecker, W. Keusgen, and J. Hillebrand, "Measurement-based investigation of 60 GHz broadband transmission for wireless in-car communication", in the 2009 IEEE 70th Vehicular Technology Conference Fall, 20-23 Sept, 2009 Anchorage, AK, USA.

[10] G. Zhu, D. Guidotti, F. Lin, Q. Wang, J. Cui, Q. Wang, L. Cao, T. Ye, and L. Wan, "Millimeter-wave inter-chip communication", in proceedings of 2012 5th Global Symposium on Millimeter-Waves, pp. 471–476, 27-30 May, 2012 Harbin, China.

[11] R. Hersyandika, "Characterization of human blockage in 60 GHz communication", M.Sc thesis, Delft University of Technology, Netherlands, Nov. 2016.

[12] 11-09-0854-03-00ad-implementation-of-60ghz-wlan-channel-model.doc

[13] A. Saleh and R. Valenzuela, "A statistical model for indoor multipath propagation," IEEE Journal on Selected Areas in Communications, Vol. 5, No. 2, pp. 128-137, 1987.

[14] Y. S. Cho, J. Kim and W. Y. Yang, MIMO-OFDM wireless communications with MATLAB, 31, Wiley Publishing, November, 2010.

[15] L. J. Greenstein, S. S. Ghassemzadeh and V. Erceg, "Ricean K-Factors in narrow-band fixed wireless channels: Theory, experiments, and etatistical models', IEEE Transactions on Vehicular Technology. Vol. 58, No. 8, pp. 4000-4012, 2009.

[16] A. Karttunen, K. Haneda, J. Jarvelainen, and J. Putkonen, "Polarisation characteristics of propagation paths in indoor 70 GHz channels," in the 2015 9th European Conference on Antennas and Propagation (EuCAP), 13-17 April, 2015 Lisbon, Portugal.

[17] F. Yıldırım, Ali S. Sadri, and H. Liu, "Polarization effects for indoor wireless communications at 60 GHz', IEEE Communication Letter, vol. 12, pp. 660–662, 2008.

[18] C. Gustafson, K. Haneda, S. Wyne and F. Tufvesson, "On mm-wave multipath clustering and channel modeling", IEEE Transactions on Antennas and Propagation, Vol. 62, No. 3, pp. 1445-1455, 2014.

[19] A .K. M. Baki, S. Sharmin, Effect of radiation patterns on WLAN delay spreads for 60 GHz living room environments, in the 2017 IEEE International Conference on Telecommunications and Photonics (ICTP), pp. 61-71, 26-28 December, 2017 Dhaka, Bangladesh.

[20] E. Perahia and R. Maslennikov, IEEE doc. 802.11-09/0499r1, Simulation scenario floor plans, May 9, 2009.

[21] E. Perahia, IEEE doc. 802.11-10/0296r14, TGad evaluation methodology, Jan. 20, 2010.

[22] G. L. Turin, "Communication through noisy, random-multipath channels," in IRE Conven. Rec., pp. 154–166, pt. 4, 1956.

[23] G. L. Turin, F. D. Clapp, T. L. Johnston, S. B. Fine and D. Lavry, A statistical model for urban multipath propagation, IEEE Transactions on Vehicular Technology, Vol. 21, No. 1, pp. 1-9, 1972.

[24] A. F. Molisch, J. R. Foerster, and M. Pendergrass, "Channel models for ultrawideband personal area networks," IEEE Wireless Communication, Vol. 10, No. 6, pp. 14–21, 2003.

[25] J. R. Foerster, "Channel modeling subcommittee report final," Tech. Rep. P802.15 02/490r1, IEEE 802.15 SG3a, Feb. 2003.

[26] M. Pendergrass, "Empirically based statistical ultra-wideband channel model," IEEE P802.15-02/240-SG3a.

[27] P. F. M. Smulders and L. M. Correia, "Characterisation of propagation in 60 GHz radio channels", Electronics and Communication Engineering Journal, Vol. 9, No. 2, pp. 73-80, 1997.

[28] The Federal Communications Commision website. [Online]. Available: https://www.fcc.gov/2004-wireless-broadband-forum-comments-received/.

[29] T. Rappaport, Wireless Communications: Principles and Practice, 2nd ed., Prentice Hall PTR, Upper Saddle River, NJ, USA, 2001.

[30] P. F. M. Smulders, "Statistical characterization of 60-GHz indoor radio channels", IEEE Transactions on Antennas and Propagation, Vol. 57, No. 10, pp. 2820-2829, 2009.

[31] K. Chandra, A. Doff, Z. Cao, R. V. Prasad and I. Niemegeers, "60 GHz MAC standardization: Progress and way forward," in the 2015 12th Annual IEEE Consumer Communications and Networking Conference (CCNC)*, pp. 182-187, 9-12 January, 2015 Las Vegas, NV, USA.

Authors' Profiles

Shaela Sharmin received her B.Sc. degree in Electrical and Electronic Engineering (EEE) from the Ahsanullah University of Science and Technology (AUST), Dhaka, Bangladesh in 2015, where she is currently a Faculty Member with the Department of Electrical and Electronic Engineering. She has been pursuing her M.Sc. degree in EEE from the same University. Her research interests include Wireless Communications, Digital Signal Processing, Cyber Security, and Smart Grid.

Shakil Mahmud Boby received the B.Sc. degree in Electrical and Electronic Engineering (EEE) from the Khulna University of Engineering and Technology (KUET), Khulna, Bangladesh in 2018. Currently, he is serving Noakhali Science and Technology University (NSTU), Noakhali, Bangladesh, as a Faculty Member with the Department of Electrical and Electronic Engineering (EEE). He has been pursuing his M.Sc. degree in EEE from KUET, Khulna, Bangladesh. His research interests include Wireless Communications, Image Processing, 2-D Electronic Devices and Nanotechnology.